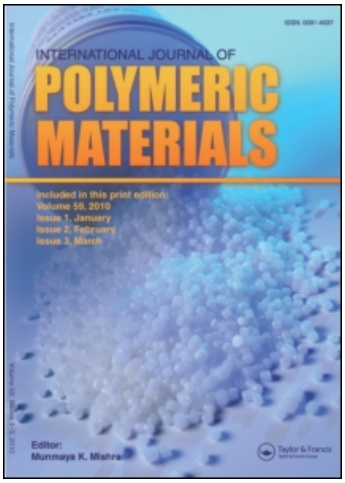

International Journal of Polymeric Materials
Publication details, including instructions for authors and subscription information:
http://www.informaworld.com/smpp/title~content=t713647664

Effect of Zone Drawing, Zone Annealing and Annealing at Constant Length on the Structure and Mechanical Properties of Biends of PET, PBT and Polyamide 6

M. Evstatiev[a]; A. A. Apostolov[a]; S. Fakirov[a]
[a] Laboratory on Structure and Properties of Polymers, Sofia University, Sofia, Bulgaria

To cite this Article Evstatiev, M. , Apostolov, A. A. and Fakirov, S.(1999) 'Effect of Zone Drawing, Zone Annealing and Annealing at Constant Length on the Structure and Mechanical Properties of Biends of PET, PBT and Polyamide 6', International Journal of Polymeric Materials, 43: 3, 207 — 232
To link to this Article: DOI: 10.1080/00914039908009686
URL: http://dx.doi.org/10.1080/00914039908009686

Intern. J. Polymeric Mater., 1999, Vol. 43, pp. 207–232
Reprints available directly from the publisher
Photocopying permitted by license only

Effect of Zone Drawing, Zone Annealing and Annealing at Constant Length on the Structure and Mechanical Properties of Blends of PET, PBT and Polyamide 6

M. EVSTATIEV *, A. A. APOSTOLOV and S. FAKIROV

Laboratory on Structure and Properties of Polymers,
Sofia University, 1126 Sofia, Bulgaria

(Received 17 March 1998)

Binary (1:1 by wt.) and ternary (1:1:1 by wt.) blends of polyethylene terephthalate, poly(butylene terephthalate) and polyamide-6 were extruded as strips and ultraquenched from the melt. After zone drawing and subsequent zone annealing or annealing at constant length at temperature $T = 220°C$ for 5 hours in vacuum, the samples were studied by differential scanning calorimetry, wide-angle X-ray scattering, small-angle X-ray scattering and mechanical testing. Substantial improvement of the mechanical properties (increase of Young's modulus and tensile strength) was established after zone annealing, compared to the annealing at constant length. Some proofs are given in the case of zone annealed samples for partial chain unfolding in the crystalline regions and maximal stretching of macromolecules in the non-crystalline regions, *i.e.*, an increase in the number of taut tie molecules is achieved. This leads to a significant improvement of the mechanical properties. Exchange reactions and creation of copolymer layers at the interface between the parent polymers, are believed to occur during the annealing at constant length, playing the role of selfcompatibiliziers. These layers suppress the separation of the homopolymers under the action of external mechanical strains or simply upon aging.

Keywords: PET; PBT; PA-6; polymer blend; zone drawing; zone annealing

* Corresponding author.

INTRODUCTION

It is known that the most common approaches to the preparation of high performance polymer materials deal with the transformation of the isotropic structure into an anisotropic (highly oriented) one. This change in the supermolecular organization is achieved most often by cold or warm drawing, solid state extrusion, superdrawing, high-speed melt spinning, zone drawing and zone annealing. The so called method of "zone annealing" has been proposed by Kunugi *et al.* [1–3] and consists of two stages, namely zone drawing and the real zone annealing. During the first stage, the amorphous or slightly crystalline films or fibers are being oriented under relatively low stress by the passage of a heater (with temperature below the crystallization temperature of the polymer) along their surface. In the second stage the material is subjected to zone annealing under high stress at temperature assumed to be the most appropriate for the crystallization of the polymer. The real zone annealing is carried out by several passages of the heater along the surface of the already zone drawn material. Due to the combined action of stress and heat on a very narrow (about 1 mm) portion of the sample, additional extension, alignment and orientational crystallization in the axial direction of the chains occurs. Very high performance polymer materials based on polyolefins or linear polycondensates are obtained by means of this method [1–3]. In our previous studies [4–7], we obtained and investigated samples by zone drawing, followed by annealing at constant length of binary or ternary blends of poly(ethylene terephthalate) (PET), poly(butylene terephthalate) (PBT) and polyamide-6 (PA). It was established that at high annealing temperatures, close to the melting ones, physical processes like crystallization, relaxation and melting take place simultaneously with some chemical processes like solid state exchange and condensation reactions. Whereas the physical processes improve the perfection of the crystallites, the chemical reactions result in the formation of copolymers. Both processes lead to an improvement of the mechanical properties of the blends. It should be noted that the occurrence of chemical reactions is enchanced to a great extend at temperatures close to the melting point of at least one of the components of the system and the copolymers formed influence substantially the structure and crystallization ability of the blends.

The present investigation aims to follow and distinguish between the changes in the supermolecular organization and mechanical properties of sample thermally treated by three different ways, namely: 1) zone drawn samples, referred here as ZD; 2) zone drawn and subsequently zone annealed samples, referred here as ZA and 3) samples undergone zone drawing and subsequent annealing at constant length (annealing at constant length), referred here as CL. Chemically the samples represent PET, PBT and PA. An attempt is made to establish some relationship between the respective structures caused by the three types of thermal treatment, the chemical composition of the blends and their properties.

EXPERIMENTAL

The polymers used were PET (Merge 1934F, Goodyear, $\overline{M}_n = 23400$), PBT (RE6131, DuPont, $\overline{M}_n = 21300$) and PA (Capron 8200, Allied Co., $\overline{M}_n = 20600$). After cooling in liquid nitrogen they were finely ground to obtain a powder and then mixed in the solid state in a ratio of 1:1 by wt. for all three binary blends and in a ratio of 1:1:1 by wt. for the ternary blend. In order to obtain films of the homopolymers and of the blends a capillary rheometer, flushed with argon and heated to about 280°C, was loaded with powdered material. The melt obtained was kept in the rheometer for 5–6 min and then extruded through a nozzle (1 mm diameter) on metal rolls rotating at about 30 rpm. The rolls were immersed in a quenching bath of liquid nitrogen. In this way films of homopolymers and all four blends were prepared, their thickness (0.10–0.15 mm) and width (4–5 mm) depending on the extrusion rate and distance between the rolls. It was established, by X-ray and calorimetric studies, that immediately after quenching, PET and PET/PBT blends were completely amorphous while the films of the PA containing blends were partially crystalline.

All samples were oriented by zone drawing under the following conditions: as quenched films under tension of 15 MPa were subjected to the action of a heating zone, using a specially devised heater (glass tube, diameter of 3 mm, containing a metal heating element). The heater was attached to the crosshead of an Instron machine for

mechanical testing and moved from the lower to the upper part of the films under tension at a crosshead speed of 10 mm/min. The temperature of the heating zone was 180°C for PA, PET/PA, PBT/PA and PET/PBT/PA blends and as low as 85°C for PET, PBT and their blend, since at higher temperatures these samples broke. Thus, ZD samples were obtained. In order to obtain ZA samples, ZD ones were subsequently zone annealed, using the same facility as that for zone drawing. Both the temperature of the heater and the tension applied to the films during zone annealing were much higher (T_a = 220°C, tension 150 MPa) than those in the case of zone drawing. The zone annealing cycle was repeated up and down 5 times at a crosshead speed of 100 mm/min. After the zone annealing the samples were extended additionally in comparison to the ZD ones. In order to obtain CL samples, ZD ones were subsequently annealed at constant length at 220°C for 5 hours in vacuum. These preparation conditions are given in Table I together with the draw ratio after the zone drawing λ and the final degree of drawing after the zone annealing or the annealing at constant length λ_{end}. The ZA samples PET/PBT, PET and PBT are not included in the table as they broke during the zone annealing.

DSC measurements were carried out on a Perkin–Elmer 2C thermoanalyzer at a heating and cooling rate of 10°C/min. The sample was heated in the calorimeter cell from 60 up to 300°C. Next, the sample was kept at 290°C for 1 min and a subsequent non-isothermal crystallization upon cooling down to 70°C from the melt was performed. The sample thus crystallized was subjected to a second heating alike the first one. Thermograms were taken during the first and second heating, when the sample melted, as well as during the cooling, when the sample crystallized. The enthalpy of fusion of the first (ΔH_f) and the second ($\Delta H_f'$) melting as well as the enthalpy of non-isothermal crystallization from the melt (ΔH_c) of the homopolymers in the blends were obtained from the DSC curves. The DSC-degree of crystallinity w_c of the homopolymers in the blends was determined according to the equation $w_c = \Delta H/F\Delta H_o$ where ΔH is the measured heat of fusion, F is the homopolymer weight fraction in the respective blend (0.5 for the binary and 0.333 for the ternary blend) and ΔH_o = 140 kJ/kg [8], ΔH_o = 144.5 kJ/kg [9] and ΔH_o = 230 kJ/kg [10]) are the ideal heats of fusion of PET, PBT and PA, respectively.

TABLE I Sample preparation conditions. Zone drawing: one passage of the heater with a rate of 10 mm/min at 15 MPa tension; zone annealing: five passages of the heater with a rate of 100 mm/min at 150 MPa tension. T_a-annealing temperature at constant length and t_a-annealing time

Sample	*Zone drawing temperature* (°C)	*Draw ratio* λ	*Zone annealing temperature* (°C)	*Annealing in vacuum at constant length* T_a(°C)	t_a(h)	*Final draw ratio* λ_{end}
PET/PBT-ZD	85	4.3	–	–	–	4.3
PET/PBT-CL	85	4.3	–	220	5	4.3
PET/PA-ZD	180	4.2	–	–	–	4.2
PET/PA-ZA	180	4.2	220	–	–	5.6
PET/PA-CL	180	4.2	–	220	5	4.2
PBT/PA-ZD	180	4.0	–	–	–	4.0
PBT/PA-ZA	180	4.0	220	–	–	4.0
PBT/PA-CL	180	4.0	–	220	5	4.0
PET/PBT /PA-ZD	180	4.5	–	–	–	4.5
PET/PBT /PA-ZA	180	4.5	220	–	–	6.0
PET/PBT /PA-CL	180	4.5	–	220	5	4.5
PET-ZD	85	4.0	–	–	–	4.0
PET-CL	85	4.0	–	220	5	4.0
PBT-ZD	85	3.8	–	–	–	3.8
PBT-CL	85	3.8	–	220	5	3.8
PA-ZD	180	3.8	–	–	–	3.8
PA-ZA	180	3.8	200	–	–	4.2
PA-CL	180	3.8	–	220	5	3.8

All X-ray measurements were performed using Ni-filtered CuK_α-radiation from a generator "Kristalloflex" of Siemens, FRG. WAXS equatorial and near-meridional diffraction patterns were obtained using Siemens diffractometer D500. Scherrer's formula [11] was used in order to calculate the crystallite size from the halfwidth of certain reflections. The crystallite size of the crystallites in the axial direction was assessed from the near meridional reflections ($\bar{1}$ 05) of PET and ($\bar{1}$ 04) of PBT, while that in the lateral direction was determined from the equatorial scan of the respective (010) reflections. The (200) reflection of PA (α-form) was used to obtain the PA crystallite size.

In order to estimate the orientation of the macromolecules with respect to the fiber axis, azimuthal profiles of the reflections ($\bar{1}$ 05) and ($\bar{1}$ 04) of PET and PBT, respectively, were obtained for all samples

containing PET or/and PBT. These profiles were taken using the diffractometer in transmission mode at a fixed angle two theta and by turning around the angle χ the sample holder in his own plane from -30 to 30 deg.

SAXS curves of the homopolymers and the blends were recorded by means of a Kratky camera equipped with detector. The long spacing L was calculated from these curves using the Bragg's law.

Mechanical tests in a static mode were carried out on a Zwick 1464 machine equipped with an incremental extensometer at room temperature and crosshead speed of 5 mm/min. Young's modulus E (in the deformation range 0.05 to 0.5 %), the tensile strength σ as well as the relative deformation at break ε were determined from the stress-strain curves. All values were averaged from five measurements.

The density was measured at 23°C by the flotation method using a carbon tetrachloride/*n*-heptane mixture.

RESULTS

Thermal Behavior

Figures 1 and 2 show DSC curves of the first melting of ZD, ZA and annealed at constant length films of PET/PBT and PET/PA, as well as of PBT/PA and PET/PBT/PA blends, respectively. The ZD samples do not show peaks of cold crystallization, which means that the homopolymers in these samples have already crystallized during the zone drawing. The PET/PBT and PET/PA blends show two well resolved melting peaks at about 220°C for PA and PBT and at 253°C for PET. These peaks are another confirmation of the relatively high crystallinity resulting from the zone drawing, regardless of the relatively low temperature of the heater for sample PET/PA (180°C) and especially for sample PET/PBT (85°C, Tab. I). Since PBT and PA have approximately the same melting temperatures of about 220°C, these components reveal a single melting peak in both the binary PBT/PA blend and the ternary one (Fig. 2). The melting peak of PET in the ternary blends appears again, as in Figure 1, at about 253°C.

Figures 1 and 2 show that the melting curves of ZA blends have almost identical trends in comparison with those of the respective ZD

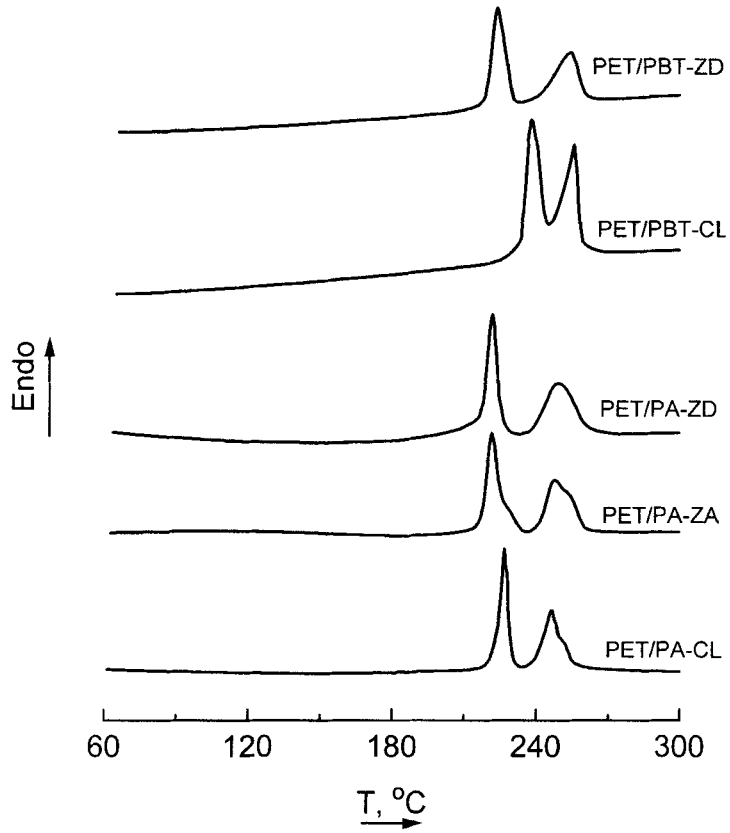

FIGURE 1 DSC curves of the first melting of ZD, ZA and annealed at constant length films of PET/PBT and PET/PA blends.

blends, suggesting in this way that zone annealing does not cause substantial changes in the crystalline structure of the hompolymers. In order to obtain more precise information, some structural parameters as density ρ, melting temperature T_m, enthalpy of fusion ΔH_f, degree of crystallinity w_c of the homopolymers as well as total enthalpy of fusion of the blends $\Sigma \Delta H_f$, are shown in Table II together with some identical parameters, characterizing the second crystallization (crystallization temperature T_m, total enthalpy of crystallization $\Sigma \Delta H_c$) and melting during the second heating (melting temperature T_m and total enthalpy of fusion $\Sigma \Delta H_f$'). As shown in this table, ρ, T_m, ΔH_f, w_c of the homopolymers as well $\Sigma \Delta H_f$ have almost the same values for

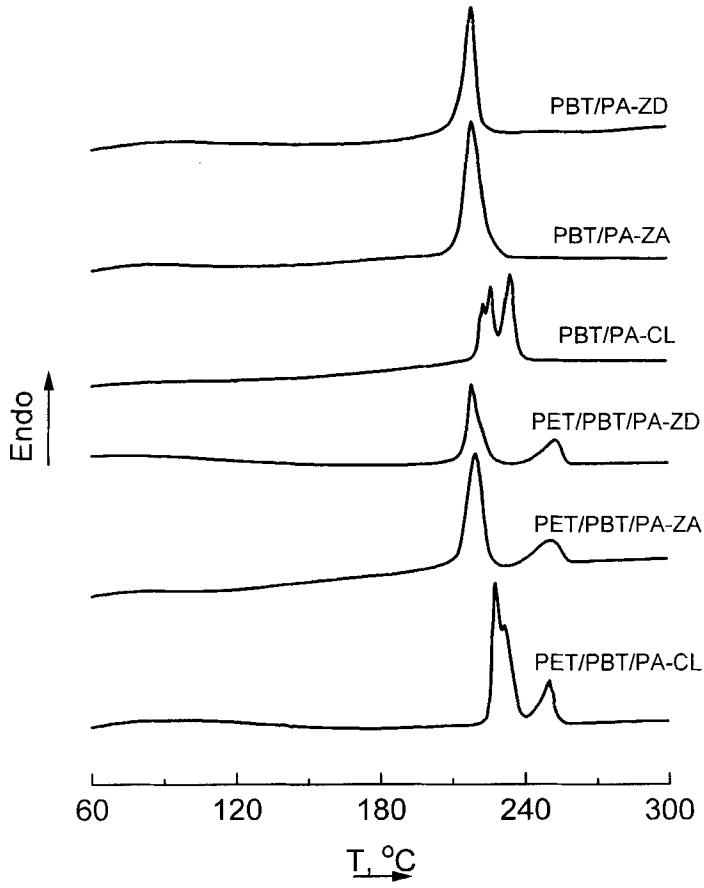

FIGURE 2 DSC curves of the first melting of ZD, ZA and annealed at constant length films of PBT/PA and PET/PBT/PA blends.

samples PET/PA-ZD and PET/PA-ZA, on the one hand, and PET/PBT/PA-ZD and PET/PBT/PA-ZA, on the other. However, considerable increase of $\Sigma \Delta H_f$ is established in the PBT/PA-ZA sample. The data of the density ρ of all blends studied (Tab. II) are another experimental indication of the irrelevant changes in the crystalline structure of homopolymers after ZA. The densities of the ZD and those of the ZA samples are practically the same for all three binary blends as well as for the ternary one. The densities of the samples, annealed at constant length, however, show relatively higher values in

comparison to the ZD samples (Tab. II). This is probably due to the more perfect structure rather than to the higher volume fraction of the crystalline phases in these samples, as seen from the w_c values (Tab. II). The sharpening of the melting peaks (doublets for samples PET/PBT-CL, PET/PA-CL and triplets for PBT/PA-CL and PET/PBT/PA-CL, Figs. 1 and 2) and the observed shift of the low-temperature melting peak to higher temperature for the annealed at constant length samples (Tab. II) also confirm that a more perfect structure is obtained as a result of annealing at constant length. What is more, Table II shows that the enthalpy of fusion and the degree of crystallinity of the homopolymers in annealed at constant length samples (PET/PBT-CL, PET/PA-CL and PET/PBT/PA-CL) show values that are relatively higher than those in the case of ZA. The same holds also for the total enthalpy of fusion of these blends, while the value of $\Sigma \Delta H_f$ for sample PBT/PA-CL is lower than that of sample PBT/PA-ZA (Tab. II). Probably due to the higher crystallization ability of PBT and PA, the contribution of these components to the magnitude of $\Sigma \Delta H_f$ is considerably greater than that of the PET component (Tab. II).

Figures 3 and 4 show DSC curves of non-isothermal crystallization upon cooling from the melt of all ZD, ZA and annealed at constant length blends. The ZD and ZA samples of one and the same blend show curves of identical trend. Sample PET/PA (Fig. 3) and samples PBT/PA (Fig. 4) reveal two peaks of crystallization, whereas sample PET/PBT/PA is characterized by a single one at about 185°C. Figure 3 clearly shows that the annealed at constant length blends have a broad temperature range of crystallization and that crystallization starts at lower temperatures than in the case of ZD blends. The same holds to a lesser extent for the annealed at constant length blends, as seen from the DSC curves shown in Figure 4. The temperature of crystallization T_c of the these blends is lower than that of ZD ones (Tab. II). Furthermore, the values of the total enthalpy of crystallization $\Sigma \Delta H_c$, as evaluated from Figures 3 and 4, of all annealed at constant length blends (Tab. II) are lower than those of the ZA blends. All these results illustrate unambiguously the decreased crystallization ability of the annealed at constant length samples.

DSC curves of the second melting of the blends crystallized from the melt are presented in Figure 5. One may note the absence of peaks of cold crystallization in all blends, the similar trends and shapes of the

TABLE II Density and DSC data of zone drawn, zone annealed and annealed at constant length PET/PBT, PET/PA, PBT/PA (1:1 by wt.), PET/PA/PBT (1:1:1 by wt.) blends and homopolymers PET, PA and PBT

Sample	*Density*	*First heating*				*Crystallization*		*Second heating*	
	$\rho\ (g \cdot cm^{-3})$	$T_m(°C)$	$\Delta H_f(kJ \cdot kg^{-1})$	$w_c(DSC)$	$\Sigma\Delta H_f(kJ \cdot kg^{-1})$	$T_c(°C)$	$\Sigma\Delta H_c)\ (kJ \cdot kg^{-1})$	$T_m(°C)$	$\Sigma\Delta H_f'(kJ \cdot kg^{-1})$
		PET PBT	PET PBT	PET PBT	PET + PBT		PET + PBT		PET + PBT
PET/PBT-ZD	1.352	253 221	57 48	0.41 0.33	53	166	44	209 239	38
PET/PBT-CL	1.384	254 233	66 75	0.46 0.52	71	132	30	214	23
		PET PA	PET PA	PET PA	PET + PA	PET PA	PET + PA		PET + PA
PET/PA-ZD	1.241	253 220	55 68	0.39 0.29	62	206 184	44	214 220 255	46
PET/PA-ZA	1.244	252 223	56 71	0.40 0.30	65	208 185	45	212 218 252	42
PET/PA-CL	1.275	253 228	65 88	0.46 0.38	76	194 182	37	190 214 246	34
		PBT + PA	PBT PA	PBT PA	PBT PA	PBT + PA			PBT + PA
PBT/PA-ZD	1.211	220			64	180 192	54	210 217	52
PBT/PA-ZA	1.226	225			84	180 193	73	209 217 240	62
PBT/PA-CL	1.237	222 229 237			72	180	48	210 215	48
		PET PBT + PA	PET PBT + PA	PET	PET + PBT + PA		PET + PBT + PA		PET + PBT + PA
PET/PBT/PA-ZD	1.258	253 220	55 56	0.39	56	186	47	210 217 238	34
PET/PBT/PA-ZA	1.261	254 222	57 63	0.40	62	183	48	209 217 240	33
PET/PBT /PA-CL	1.292	251 229 234	51 81	0.36	72	177	38	208 215 232	26
PET-ZD	1.358	255	58	0.41		208	42		
PET-CL	1.434	258	74	0.51		205	38		
PBT-ZD	1.292	220	66	0.45		189	50		
PBT-CL	1.356	240	72	0.50		182	44		
PA-ZD	1.127	218	75	0.32		186	56		
PA-ZA	1.130	217 224	76	0.33		186	61		
PA-CL	1.168	229	81	0.35		185	49		

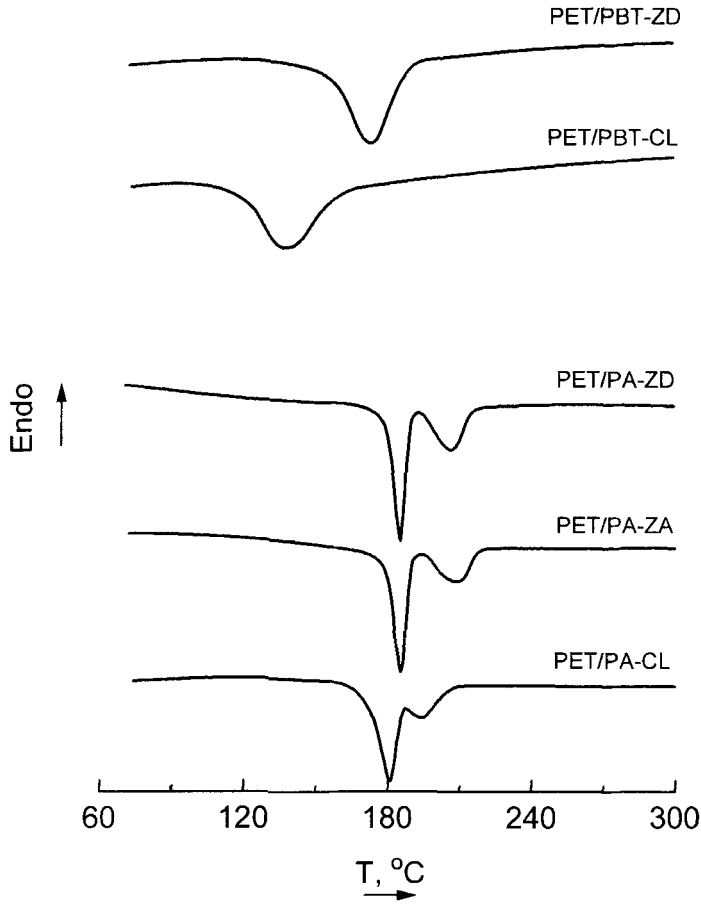

FIGURE 3 DSC curves of non-isothermal crystallization upon cooling from the melt of PET/PBT and PET/PA blends.

curves and the complete coincidence of the ranges and maxima of the melting peaks of ZD and ZA samples of one and the same composition. Practically the same total enthalpy of fusion $\Sigma \Delta H_f$ is observed with samples PET/PA-ZD and PET/PA-ZA as well as with samples PET/PBT/PA-ZD and PET/PBT/PA-ZA. Sample PBT/PA-ZA is an exception since it shows higher $\Sigma \Delta H_f$-values than samples PBT/PA-ZD and PBT/PA-CL. The other annealed at constant length blends (samples (PET/PA-CL, PET/PA-CL and PET/PBT/PA-CL),

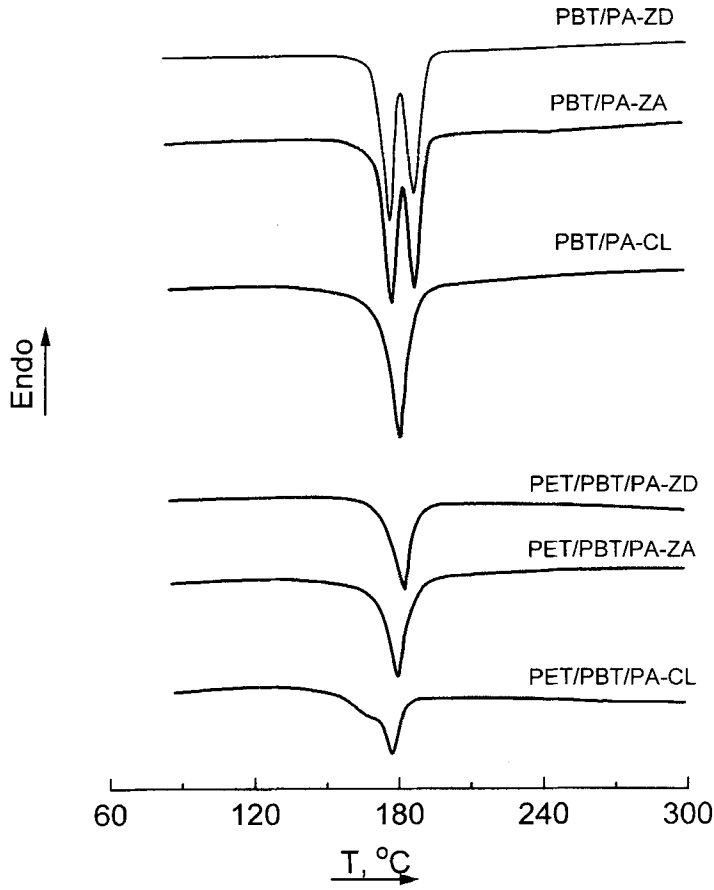

FIGURE 4 DSC curves of non-isothermal crystallization upon cooling from the melt of PBT/PA and PET/PBT/PA blends.

however, show lower values of $\Sigma \Delta H_f$ than the ZD samples (Tab. II). The melting temperatures of the polymer components in the blends are much lower during the second heating than during the first one (Tab. II). The same holds for the $\Sigma \Delta H_f$' values as compared to the $\Sigma \Delta H_f$ values (Tab. II). These two findings could be explained by the difference in perfection and quantity of crystallites of the homopolymers before the first and the second heating. Furthermore, in the case of annealing at constant length, the total enthalpy of crystallization is higher or commensurable with the total enthalpy of second

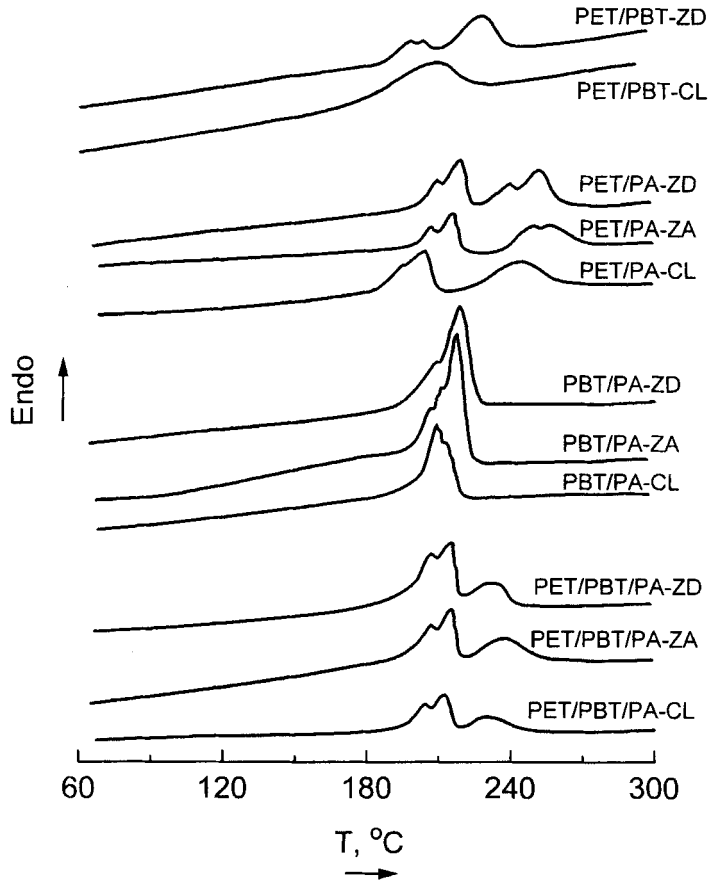

FIGURE 5 DSC curves of the second melting of the blends crystallized from the melt.

fusion (Tab. II). These considerations represent another indication of the reduced crystallization ability of the annealed at constant length blends in addition to the fact that PET is a slowly crystallizing polymer in comparison to PBT and PA.

Table II shows also DSC data obtained from the curves of melting and non-isothermal crystallization during the cooling from the melt of ZD, ZA and annealed at constant length films of the homopolymers. There is no difference in the melting temperatures as well as in the enthalpies of fusion of the PA samples, subjected to ZD and to ZA.

A substantial increase of T_m, ΔH_f and w_c is observed in the case of the annealed at constant length homopolymers, in comparison to the ZD ones. It should be noted, however, that while the enthalpies of fusion and the degrees of crystallinity of the PA and PBT components in the blends are commensurable with those of the neat homopolymers having the same thermal prehistory, the degree of crystallinity of PET in all blends is lower than that of the pure polymer (Tab. II). This is probably a result of the faster crystallization of PA and PBT in the blends and of the steric hindrance of these two components with respect to the growth of PET crystallites.

WAXS and SAXS Behavior

In order to obtain quantitative information about the effect of both types of annealing on the structure, the crystallite sizes $D\langle 010\rangle$-and $D\langle \bar{1}\,05\rangle$ for PET, $D\langle 010\rangle$ and $D\langle \bar{1}\,04\rangle$ for PBT and $D\langle 200\rangle$ for PA were obtained. In some cases the maxima were very poor and their width could not be measured accurately. The crystallite sizes are given in Table III. Since $\langle \bar{1}\,05\rangle$ for PET and $\langle \bar{1}\,04\rangle$ for PBT make approximately ten degrees with the "c"-axis, which almost coincides with the fibre axis, the respective sizes represent the lamella thickness. The lateral size D of PET crystallites was measurable only in ZA and annealed at constant length PET/PA blends and was found to be

TABLE III Some sizes of PET, PBT and PA crystallites as obtained from wide angle X-ray scattering using Scherrer's formula [11]. "+" means that the reflex has very low intensity or is overlapped by neighboring reflexes, whereas "–" means absence of the reflex due to the absence of the respective polymer in the blend

Sample	*L*, Å	*PET*		*PBT*		*PA*
		010	$\bar{1}\,05$	010	$\bar{1}\,04$	200
PET/PBT-ZD	+	+	32	+	+	–
PET/PBT-CL	115	+	42	–	38	–
PET/PA-ZD	76	+	36	–	–	+
PET/PA-ZA	128	71	43	–	–	51
PET/PA-CL	119	66	39	–	–	106
PBT/PA-ZD	98	–	–	71	27	+
PBT/PA-ZA	134	–	–	84	37	+
PBT/PA-CL	116	–	–	118	40	84
PET/PBT/PA-ZD	110	+	38	+	23	+
PET/PBT/PA-ZA	132	+	39	+	36	51
PET/PBT/PA-CL	123	+	41	+	35	84

practically the same. The PET lamella thickness $D\langle\bar{1}\,05\rangle$ rises by 30 % in PET/PBT blend after annealing at constant length, but is practically the same both after zone drawing and after annealing at constant length in PET/PA and in the ternary blend. Both the lateral size $D\langle 010\rangle$ and the lamella thickness $D\langle\bar{1}\,04\rangle$ of PBT crystallites increase significantly in PBT/PA blend after zone annealing and additionally after annealing at constant length. The lamella thickness of PBT rises in a similar way in the PBT/PA blend and in the ternary one. The size $D\langle 200\rangle$ of PA crystallites double its value after annealing at constant length in comparison to the zone annealing both of PET/PA and of the ternary blend.

The intensity profiles in azimuthal direction of the two $(\bar{1}\,05)$ reflections of PET, taken from 30 to 30 degrees χ, are shown in Figure 6. These two reflections are theoretically situated at approximately ± 10 degrees off-meridian and their separation can be used as a measure of the degree of orientation of the PET crystallites. As seen in Figure 6, all zone drawn samples containing PET reveal low degree of orientation since the two off-meridional reflections merge in one reflex at $\chi = 0$ degrees. For all ZA and annealed at constant length samples, this reflex splits into two off-meridional $(\bar{1}\,05)$ reflections. As a measure of the crystal orientation the following considerations were taken: i) the distance between the two maxima in degrees [12]- the larger the distance the higher the degree of orientation of crystallites; ii) the well known fact that the higher the degree of orientation of crystallites, the better the two $(\bar{1}\,05)$ reflections split azimuthally [13], hence the halfwidth of one $(\bar{1}\,05)$ reflection can be taken as a measure of the orientation, and iii) the fact that the lower the ratio of the intensities taken at $\chi = 0$ and $\chi(I_{max})$, where I_{max} is the intensity of the $(\bar{1}\,05)$ reflection, the higher the degree of orientation. Having in mind these considerations, it is clearly seen in Figure 6 that samples PET/PA-ZA and PET/PA-CL on the one hand, and PET/PBT/PA-ZA and PET/PBT/PA-CL on the other, have approximately the same degree of orientation of PET crystallites. Sample PET/PBT-CL shows the highest orientation of these crystallites.

Two $(\bar{1}\,04)$ reflections, theoretically situated at approximately ± 10 degrees χ off-meridian, were used to characterize the orientation of PBT crystallites in the blends, similarly to the two $(\bar{1}\,05)$ reflections in the case of PET crystallites. The intensity profiles in azimuthal

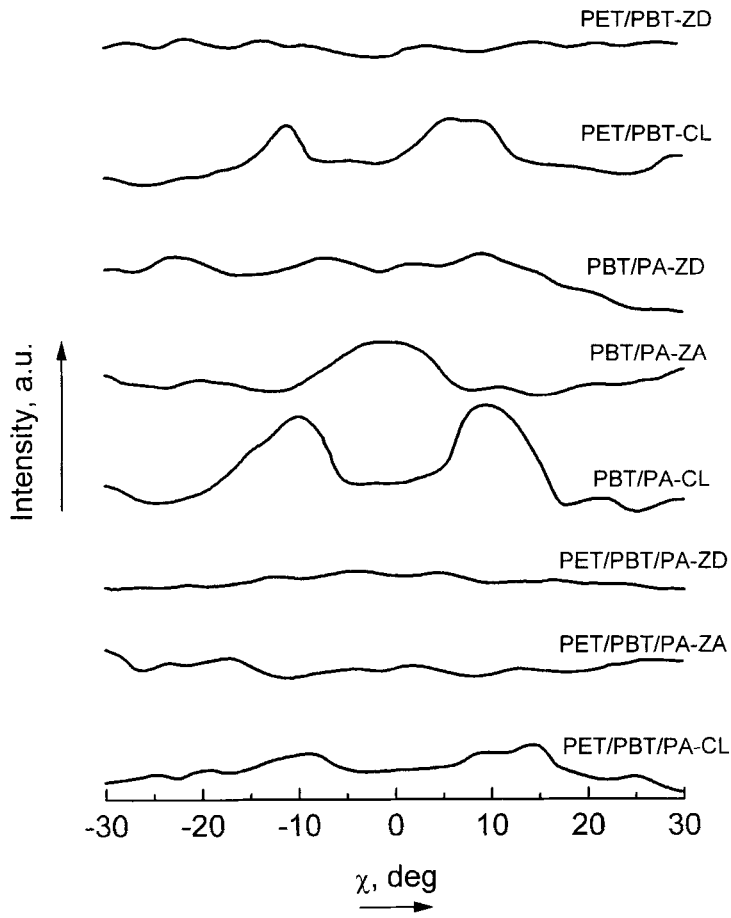

FIGURE 6 Intensity profiles in azimuthal direction of two near meridional ($\bar{1}\,04$) reflections of PBT, taken from all blends containing PBT.

direction of these two ($\bar{1}\,04$) reflections of PBT, taken from −30 to 30 degrees χ for the PBT containing blends, are shown in Figure 7. All ZD samples containing PBT do not show any preferable orientation of the PBT crystallites. The same holds for sample PET/PBT/PA-ZA. Sample PBT/PA-ZA is characterized by a low degree of orientation of PBT crystallites, as seen form the poorly expressed maximum at $\chi = 0$. The degree of orientation of the PBT crystallites in the ZD and annealed at constant length samples strongly depends on the chemical

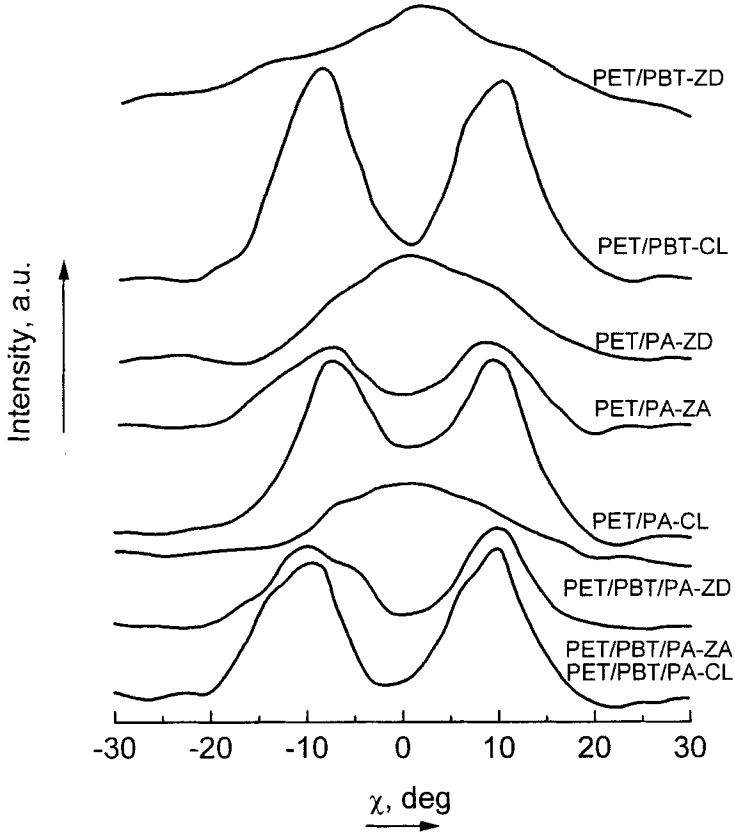

FIGURE 7 Intensity profiles in azimuthal direction of two near meridional ($\bar{1}$ 05) reflections of PET, taken from all blends containing PET.

composition, in contrast to the degree of orientation of PET crystallites, which depends mainly on the sample preparation conditions. Thus, the degree of orientation of the PBT crystallites is very low for sample PET/PBT/PA-CL, which is almost isotropic, moderate for sample PET/PBT-CL and relatively high for sample PBT/PA-CL. A comparison of Figures 6 and 7 points out that as a whole, the degree of orientation of the PBT crystallites is much lower than the degree of orientation of the PET ones. A direct comparison between the respective curves of the blends, comprising both PET and PBT (curves for the PET/PBT and PET/PBT/PA blends, Figure 6, and the respective

curves in Figure 7 leads to the conclusion that only the PET crystallites become oriented after zone drawing. In the ZD samples the temperature of the zone is far below the melting temperature of any of the components and the PET crystallites in these samples are moderately oriented (Fig. 6, PET/PBT-ZD and PET/PBT/PA-ZD) while the PBT crystallites remain randomly oriented (Fig. 7, PET/PBT-ZD and PET/PBT/PA-ZD). It seems that the deformation induced crystallization during the zone drawing enhances mainly the arrangement of the PET crystallites in the oriented state.

The orientation of PET crystallites is improved significantly after zone annealing or annealing at constant length, whereas only a low degree of orientation results from the annealing at constant length in the case of PBT. Annealing at 220°C of PBT and PA containing blends leads to an improvement of orientation due to additional crystallization in the oriented state. On the other hand, being close to the melting temperature of PA and PBT, this annealing leads to melting of small and defective oriented crystallites, thus resulting in a partial conversion of oriented PA and PBT into isotropic material. This is not the case of PET, where zone annealing as well as annealing at constant length, both at 220°C (far below the PET melting temperature of 260°C), results in a strong improvement of the degree of orientation of the PET crystallites (Fig. 6).

SAXS patterns of all ZD, ZA and annealed at constant length blends are shown in Figures 8 and 9. The wave vector $s = 2\theta/\lambda$ is on the abscissa and θ is the Bragg's angle in rad. For the interpretation of these curves, the densities of the phases present must be taken into account. These densities, in a descending order, are given in Table IV. The cited crystal densities characterize the ideal crystals. Since the real crystals include various defects, the real crystal densities are lower than the cited ideal ones. Upon annealing some of the defects leave the crystallites and move to the amorphous phase which results in an improvement of the perfection of the crystallites. For this reason higher crystal density of the respective components in ZA and annealed at constant length samples should be expected.

In order to draw semiquantitative conclusions from the SAXS data, represented in Figures 8 and 9, one must consider the so called scattering power $Q = \int I(s)s^2 ds$ rather than the peak intensity. The scattering power is connected with the mean square fluctuation of the

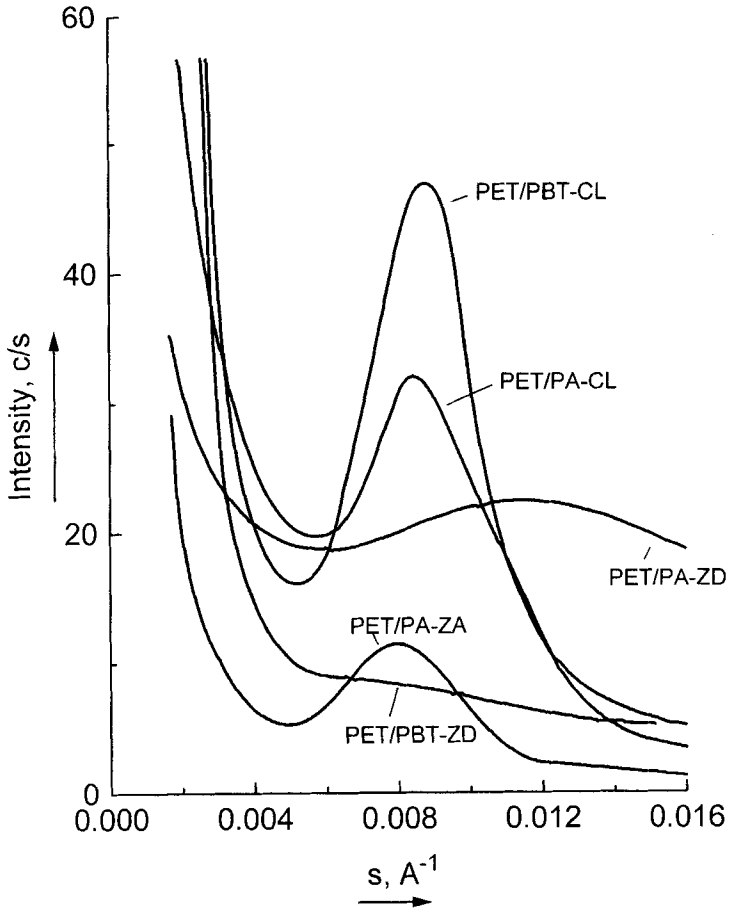

FIGURE 8 SAXS patterns of ZD, ZA and annealed at constant length PET/PBT and PET/PA blends.

electron density as $\overline{\Delta\rho^2} \sim Q$ [19] On the other hand, the mean square fluctuation of the electron density of a multicomponent system is given as [20]:

$$\overline{\Delta\rho^2} = \sum_{i,j=1}^{k} \varphi_i \varphi_j (\rho_i - \rho_j)^2 \tag{1}$$

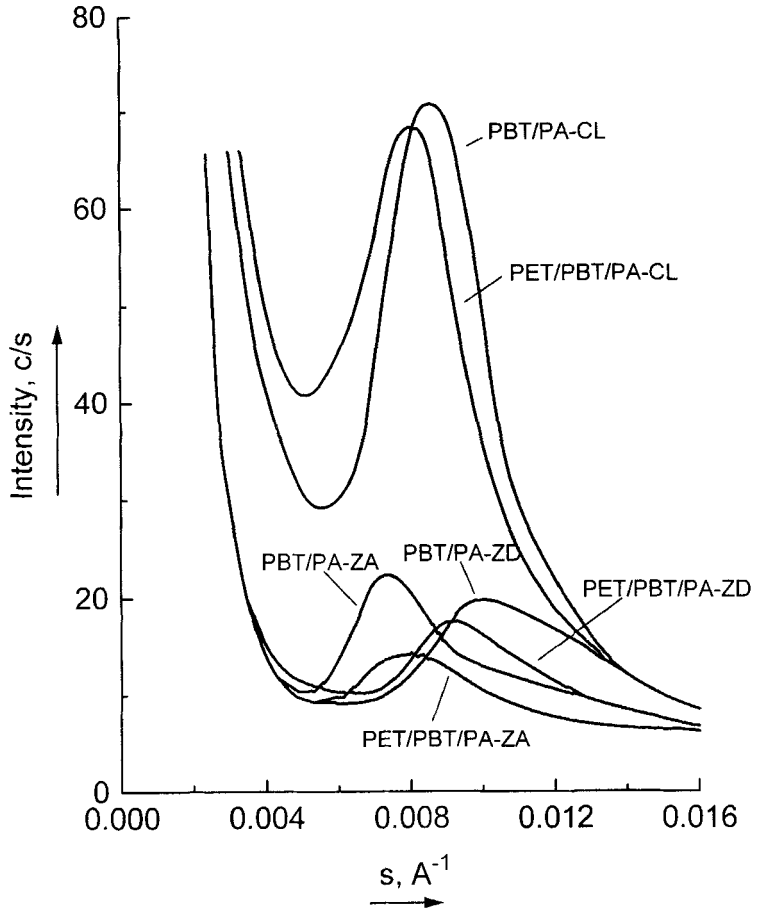

FIGURE 9 SAXS patterns of ZD, ZA and annealed at constant length PBT/PA and PET/PBT/PA blends.

TABLE IV Densities (in g/cm^3) of the crystalline and amorphous phases of the homopolymers used, in a descending order. The subscripts "*c*" and "*a*" mean crystalline and amorphous phase, respectively

ρ_c^{PET}	ρ_c^{PBT}	ρ_a^{PET}	ρ_a^{PBT}	ρ_c^{PA}	ρ_a^{PA}
1.515[14]	1.406[15]	1.335[16]	1.256[17]	1.23[18]	1.09[18]

where φ_i and ρ_i are the volume fractions and the electron densities of the i-th phase, respectively. The number of the phases k equals four for the binary blends and six for the ternary blend. The electron densities

are proportional to the densities in g/cm^3. As it can be roughly evaluated from the area under each curve in Figures 8 and 9, the Q-value for the ZA samples is of the same order of magnitude as that of the ZD samples. However, annealing at constant length (samples PET/PBT-CL, PET/PA-CL; Fig. 8 as well as samples PBT/PA-CL and PET/PBT/PA-CL, Fig. 9), leads to an abrupt increase of the Q-values. As seen from Eq. (1), the increase of $\overline{\Delta\rho^2}$ is due mostly to the increase of the largest $\Delta\rho$ differences, which in turn is caused by the increase of the highest densities (ρ_c^{PBT} in sample PBT/PA-CL and ρ_c^{PET} in the three other annealed at constant length PET samples. The relatively large width of the SAXS curves could be related to the overall contribution of the alternating structures of the two (three in sample PET/PBT/PA-CL) homopolymers with different but closely situated maxima, *i.e.*, to an effect of overlapping.

What could be the reason for the relatively low intensity of the SAXS maxima of the ZD and ZA samples in comparison to annealed at constant length ones? As seen in Table I, the temperature and especially the tension corresponding to the five-fold passage of the heater during the zone annealing are much higher than during the zone drawing. Therefore, unfolding of some of the small crystallites could occur and since the specific volume of the amorphous phase is larger than that of the crystalline phase, both the interlamellar distance and hence the long spacing should increase. This is actually the case (Fig. 8, 9) the maxima of the ZA samples lie leftward of the maxima of the ZD samples. On the other hand, although the temperature of the processes of zone annealing and annealing at constant length is the same, substantial improvement of the crystal perfection and increase of the crystal density does not occur during ZA due to the relatively short time of this process (a few minutes against to 5 hours for the annealing at constant length).

Mechanical Properties

Data on the Young's modulus E, tensile strength σ and elongation at break ε of ZD, ZA and annealed at constant length blends of PET, PBT, PA as well as of homopolymers are given in Table V. As is readily seen, zone annealing of the blends results in an increase of the Young's modulus by about 20% for samples PET/PA-ZA and PET/

TABLE V Young's modulus E, tensile strength σ and deformation ability ε of zone drawn, zone annealed and annealed at constant length PET/PBT, PET/PA, PBT/PA and PET/PBT/PA blends as well as of the homopolymers PET, PBT and PA

Sample	*E, GPa*	σ, *MPa*	ε, %
PET/PBT-ZD	8.4	237	26
PET/PBT-CL	8.9	244	30
PET/PA-ZD	9.3	330	36
PET/PA-ZA	11.1	556	11
PET/PA-CL	9.8	346	31
PBT/PA-ZD	3.7	320	30
PBT/PA-ZA	6.2	415	14
PBT/PA-CL	4.2	215	36
PET/PBT/PA-ZD	8.4	327	21
PET/PBT/PA-ZA	10.2	467	12
PET/PBT/PA-CL	8.9	336	38
PET-ZD	9.3	221	9
PET-CL	10.6	288	17
PBT-ZD	3.2	141	24
PBT-CL	4.4	156	46
PA-ZD	4.5	342	31
PA-ZA	7.0	392	18
PA-CL	4.8	312	36

PBT/PA-ZA and by about 70% for sample PBT/PA-ZA. After zone annealing the tensile strength increases by 30–40% for samples PBT/PA-ZA and PET/PBT/PA-ZA and by about 70% for sample PET/PA-ZA. The deformation ability of all ZA samples is by two to three times lower in comparison to the ZD samples. The values of E and σ for CL samples are practically the same as those for ZD samples, PBT/PA-CL being an exception, showing lower strength than sample PBT/PA-ZD. Thus, ZA samples show the highest E and σ values as well the lowest ε values.

DISCUSSION

The results from the DSC measurements, the data on the crystallite sizes and orientation, obtained by X-ray studies, clearly suggest that a direct relationship exists between the supermolecular organization and the mechanical properties of the blends under investigation. Thus for instance, the relatively high values of the Young's modulus and tensile strength of the ZD blends (Tab. V, samples PET/PBT-ZD, PET/PA-

ZD and PET/PBT/PA-ZD) are due to the relatively good orientation and alignment of the macromolecules as a result of the drawing.

On the other hand, additional thermal treatment at constant length does not result in the increase of the PET crystallite size in the longitudinal direction while the PBT crystallites in the PBT/PA blend grow both in the longitudinal and in the lateral direction (Tab. III). However, most of the reflections are either not clear enough or weak and for this reason the use of full height half-width for some reflections and samples is unreliable and even impossible. A clear increase of the long spacing is observed with the PET/PA, PBT/PA and PET/PBT/PA blends after annealing at constant length (Tab. III, compare samples PET/PA-CL and PET/PA-ZD; PBT/PA-CL and PBT/PA-ZD; PET/PBT/PA-CL and PET/PBT/PA-ZD).

The already mentioned solid state ester-exchange and condensation reactions taking place at elevated temperatures are determined by the temperature, the chemical composition of the components in the blend and the duration of the thermal treatment. These factors lead to the appearance of copolymer layers at the interface between the parent polymers, thus playing the role of selfcompatibilizers of the homopolymers, which suppress their separation under the action of external mechanical strains or simply upon aging. The slightly decreased crystallization ability of all blends as a result of annealing at constant length in comparison to that of ZD blends (Tab. II) provide an experimental proof of the formation of such copolymers. Sufficiently convincing proofs that such reactions occur are found by annealing of the blends at high temperatures (*e.g.*, 240°C) for 5 and 25 hrs [21]. The mechanical properties of the samples annealed at constant length are the same as those of the ZD samples; only in the case of sample PBT/PA-CL the tensile strength is considerably lower than that of sample PBT/PA-ZD (Tab. V). Since both polymers in this blend melt at about 225–230°C, the decrease of the strength is probably due to partial isotropization occurring upon annealing at 220°C, *i.e.*, close to the melting point of PBT and PA. As a result of this partial isotropization of the sample annealed at constant length (PBT/PA-CL) the number of tie molecules is diminished and hence the tensile strength decreases.

Let us now consider the ZA samples which have considerably better mechanical properties than the samples annealed at constant length (Tab. V, samples PET/PA-ZA, PBT/PA-ZA and PET/PBT/PA-ZA).

The ZA blends have commensurable or smaller crystallite sizes (Tab. III) as well as lower degree of orientation of PET crystallites (Fig. 6) as compared to the annealed at constant length samples. Furthermore, solid state ester-exchange and condensation reactions cannot be expected to occur upon zone annealing, since at each passage of the heater along the surface of the sample, slippage of molecules takes place. All these considerations lead to the assumption that the improved mechanical properties of the ZA samples depend to a great extent on the structure of the non-crystalline (amorphous) regions of the polymers. Due to the combined action of high temperature (220°C) and high stress (150 MPa) on a very narrow fraction of the drawn samples during the ZA, partial destruction of the lower melting PA and/or PBT components could take place as a result of chain unfolding together with the perfection of the crystallites and formation of a fibrillar structure. Thus, the relative fraction of chains under strain in the non-crystalline parts of the homopolymers (taut tie molecules) grows substantially, which leads in turn to an increase of E and σ and to the decrease of ε of the ZA samples in comparison to the ZD ones. Additional indications of the occurrence of these processes are: (i) the observed lower (by several times) SAXS intensity of ZA blends (Figs. 8 and 9); (ii) the relatively low degree of crystallinity (Tab. II); (iii) the higher drawability of the ZA blends (Tab. I); (iv) the lesser degree of orientation of the PBT crystallites in the ZA blends in comparison to annealed at constant length samples (Fig. 7) and v) the relatively high values of the long spacing of the ZA samples (Tab. III).

It should be noted that trans-(exchange) reactions have also definite contribution to the perfection of the structure in the amorphous regions and on the increase of the number of chains under strain. The existence of a great number of defects (mainly chain entanglements) in the non-crystallizable fractions of the fibrillized homopolymers as well as the conditions of zone annealing (high temperatures and stresses) favor the occurrence of these reactions. This effect is observed also by other authors [22]. Due to the very high stress during zone annealing and the subsequent slippage of highly oriented PET fibrils with respect to the additionally oriented lower melting components (PBT and/or PA), trans-reactions could occur solely between the intrafibrillar chains (*i.e.*, chains which form one and the same fibril) of the homopolymers. The formation of copolymer layers between the components

of the blend is hardly possible during the zone annealing; which is confirmed also by the observed pull out effect and cleavage upon mechanical testing of ZA samples. We found a similar phenomenon in highly oriented PET films ($\lambda = 15-18$) subjected additionally to zone annealing [21]. Cleavage was however not observed with the samples annealed at constant length.

CONCLUSIONS

During zone annealing of binary and ternary blends of polyesters (PET, PBT) and PA, structural reorganization take place and contribute to an increase of the amount of the chains under strain. In this way, zone annealing leads to a substantial improvement of the mechanical properties (Young's modulus and tensile strength) as well as to a decrease of the deformation ability, compared to both zone drawing and annealing at constant length. In contrast to zone annealing, formation of copolymer layers occurs during annealing at constant length. This compatibilization leads to better integrity of the fibers.

Acknowledgements

The authors acknowledge the partial support of DFG, FRG (Grant DFG-FR 675/21-1) as well as to the Bulgarian Ministry of Science, Education and Technology under contract X-542.

References

[1] Kunugi, T., Suzuki, A. and Hashimoto, M. (1981). *J. Appl. Polym. Sci.*, **26**, 213.
[2] Kunugi, T. (1996). Preparation of Highly Oriented Fibres or Films with Excellent Mechanical Properties by Zone-Drawing/Zone-Annealing Method, In: Oriented Polymer Materials, Ed. Fakirov, S. Huethig and Wept Verlag Zug, Heildelberg, p. 394.
[3] Kunugi, T., Ichinose, C. and Suzuki, A. (1986). *J. Appl. Polym. Sci.*, **31**, 429.
[4] Evstatiev, M. and Fakirov, S. (1992). *Polymer*, **33**, 877.
[5] Fakirov, S., Evstatiev, M. and Schultz, J. (1992). *Polymer*, **34**, 4669.
[6] Evstatiev, M., Petrovich, S. and Fakirov, S. (1993). *Macromolecules*, **26**, 5219.
[7] Fakirov, S. and Evstatiev, M. (1993). Interfacial Chemical Interactions in Condensation Polymeric Composites, In: The Interfacial Interactions in Polymeric Composites, Ed. Akovali, G. NATO-ASI, E 230, p. 417.

[8] Wunderlich, B. (1979). *Polym. Eng. Sci.*, **18**, 431.
[9] Privalko, V. P.(1984). *Handbook of Polymer Physical Chemistry*, Properties of Block Polymers, Naukova Dumka, Kiev **2**, 177 (in Russian).
[10] Gogolewski, S. and Pennings, A. I. (1977). *Polymer*, **18**, 654.
[11] Klug, H. P. and Alexander, L. E. (1974). X-ray Diffraction Procedures for Polycrystalline and Amorphous Materials, John Wiley and Sons, New York, p. 511.
[12] Bhatt, G. M., Bell, J. P. and Knox, J. R. (1976). *J. Polym. Sci. Polym. Phys. Ed.*, **14**, 373.
[13] Itoyama, K. (1987). *J. Polym. Sci. Polym. Lett.*, **25**, 331.
[14] Fakirov, S., Fischer, E. W. and Schmidt, G. F. (1975). *Makromol. Chem.*, **176**, 2459.
[15] Mencik, Z. (1975). *J. Polym. Sci. Polym. Phys. Ed.*, **13**, 2173.
[16] Kilian, H. G., Halboth, H. and Jenkel, E. (1960). *Kolloid Z. Z. Polym.*, **172**, 166.
[17] As [9], p. 150.
[18] Sweeny, W. and Zimmerman, J. (1969). In: Encyclopedia of Polymer Science and Technology, John Wiley and Sons, New York, Vol. 10, 537.
[19] Kratky, O. (1982). Natural High Polymers in the Dissolved and Solid State, In: Small Angle X-ray Scattering (Glatter, O. and Kratky, O. Eds.), Academic Press, London, p. 383.
[20] Stern, F. (1955). *Trans. Far. Soc.*, **51**, 430.
[21] Evstatiev, M., Fakirov, S., Apostolov, A. A., Hristov, H. and Schultz, J. (1992). *Polym. Eng. Sci.*, **32**, 964.
[22] Dubner, W. S. (1990). *Ph.D. Thesis*, University of Delaware.